New methods for proportional-integral controller design for time-delay systems

Aye Taiwo Ajiboye, Jayeola Femi Opadiji, Abdulrahman Olalekan Yusuf, Olusogo Joshua Popoola, Esther Toyin Olawole, Olalekan Femi Adebayo
Department of Computer Engineering, Faculty of Engineering and Technology, University of Ilorin, Ilorin, Nigeria

Article Info	ABSTRACT
	The development of structured methods for proportional-integral (PI) controller design for systems with time delay are proposed in this article. Several PI controller design methods for time-delay systems have been reported. However, combining two or more methods to form new ones have not been given serious attention. The system stability region in the controller parameters space was determined by plotting the stability boundaries. In this study, the controller gains were first obtained using genetic algorithm (GA), weighted geometric center (WGC), and centroid of convex stability region (CCSR). Thereafter, these gains were combined by finding the centroids of lines joining any of the two gain locations, and triangle whose vertices are the location of the three gains in the convex stability region, thus yielding four additional methods, M1, M2, M3, and M4. Compared to a particular existing method, some of the proposed methods yield faster response speed at the expense of reference input tracking, while the reverse is the case for others. Any of the proposed methods (M1, M2, M3, and M4) can be selected depending on the system performance specifications. *This is an open access article under the <u>CC BY-SA</u> license.*

Corresponding Author:

Aye Taiwo Ajiboye
Department of Computer Engineering, Faculty of Engineering and Technology, University of Ilorin
Ilorin, Nigeria
Email: ajiboye.at@unilorin.edu.ng

1. INTRODUCTION

Many practical control systems are modelled as time-delay system because of the negative effects of time delay on their normal operations [1]-[3]. Time delay can arise from signal processing overhead incurred by the system components and signal transmissions in the control loop [4], [5]. Therefore, designing a controller for this class of system requires full knowledge of how the system performance can be adversely influenced by time delay, and even be distabilised in worst case [6]. Among the innovations that contributes to the field of instrumentation and control in the 20th century, proportional integral derivative (PID) controller was rated second [7]. PID controllers are commonly used in industrial applications [8] due to their popularity [9], simple algorithm [10]-[13], robustness [12], [14], [15], simple design methodology and effectiveness in system control [16]. Most a time PID controller is implemented in the form of proportional-integral (PI) because its derivative component is not normally use [17].

The first step in the PI controller design for systems with time delay is establishing the system's stability boundary in the space of controller parameters [18], being the most common modern method in this type of controller design [19]. To design PI controller for time-delay system, [19] proposed a method that was based on plotting the stability boundary locus in controller parameters plane and then use the centroid of convex stability region (CCSR) method for determining the appropriate controller gains. The superiority of

this method over the existing methods was established via simulation and experiments. Consequently, analytical method for determining the CCSR in the parameter space of PI controller in the control of integrating systems with time delay [17] and unstable or stable first-order plus dead-time systems [20] were proposed. However, because of analytical approximation involved, the method sacrifices accuracy for non-repeated plotting of stability boundary locus each time new system is considered. In k_p-k_i stability region for a fixed k_d, (where k_p, k_i and k_d are proportional, integral and derivative gain respectively) was actually established for designing of PID controller, but later adopted for PI controller by allowing $k_d = 0$, to yield stability region in k_p-k_i stability region [21], [22]. Using this region and genetic algorithm (GA), optimum k_p and k_i were determined. A PI controller design method, which involves determination of system stability region in the controller parameters space and the centroid of the region was developed by [23]. The required controller is the coordinate of the centroid of the determined region. The method is simple, gives good time domain performance, and saves implementation time, compared with some common methods.

In the design of PI-PD for time-delay systems by [24], the inner PD loop was designed by determining the k_p-k_d stability region, weighted geometric center (WGC) method was used to find the controller gains within the region and based on these gains, the loop was reduced to a single block. After the reduction of the inner loop, the PI was then designed in the k_p-k_i stability region via WGC. The method is simple, robust and gives good performance compared to available methods in the literature. Onat [25] proposed a method of PI design that involved determination of k_p-k_i stability region and then calculated the WGC of the region whose coordinate values were the required gains. From the simulation results, the method yielded good compromise among the TDPMs. A method of PI controller design which rely on generating the system stability region in the k_p-k_i plane and then calculate the region WGC was present by [23]. This method is simple and reliable which make it to be very useful for control system designers.

Several methods of PI controller design for time-delay systems have been proposed in the literature. But the process of combining two or more of these methods to form new ones have not been given serious research attention, therefore the motivation for this study. The aim of this study is to develop new structured methods of PI controller design for systems with time delay from existing methods.

Combining existing methods of PI controller design to produce new methods will increase the number of methods in the PI controller design methods pool from which one can select. Also, depending on the system specification requirements, controller may be found in the new methods that will perform better than those in the existing methods. In view of these assumptions, the equations for the generation of stability region in the controller parameter space were derived. Using these equations and the critical frequency (ω_c), the system stability boundaries were plotted. Based on the stability region, GA, WGC, and CCSR methods were used for designing PI controllers in the k_p-k_i convex stability region. The resulting controller gains from these methods were then combined in four different ways. Each of these ways stand for a new method and yielding four additional methods at the end. Making these methods depend solely on the results obtained from the existing methods.

The existing and proposed methods were tested via simulation using unit step response. Considering the resulting system TDPMs value from the 3 examples used for demonstration, the proposed methods add to PI controller design methods pool. Also, some of the proposed methods outperformed some of the existing methods.

2. METHOD
2.1. Stability boundary for PI controlled system
Figure 1 shows the block diagram of unity feedback control system used for the deriving of system transfer functions. The transfer functions for the plant, time delay and controller denoted as $G_p(s)$, $G_d(s)$, and $G_c(s)$, respectively are expressed in (1), (2) and (3). Based on these equations the system closed loop response ($Y(s)$) to the input ($R(s)$) can be determined.
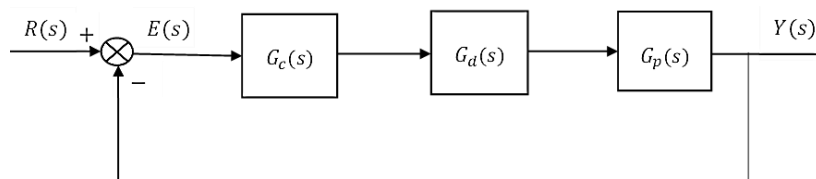

Figure 1. Block diagram of unit feedback time-delay control system

$$G_p(s) = \frac{N(s)}{D(s)} \tag{1}$$

$$G_d(s) = e^{-\tau s} \tag{2}$$

where the time delay in seconds is τ,

$$G_c(s) = \frac{k_p s + k_i}{s} \tag{3}$$

where, k_p and k_i are the proportional and integral gains, respectively.

Replacing "s" with "$j\omega$" in (1), and then to simplify the D-decomposition method, both the numerator $N(s)$ and denominator $D(s)$ of (1) were decomposed into their odd and even components as shown in (4). It should be noted that for compactness purpose $(-\omega^2)$ was removed from $N_e(-\omega^2)$, $N_o(-\omega^2)$, $D_e(-\omega^2)$ and $D_o(-\omega^2)$ in (4).

$$G_p(j\omega) = \frac{N_e + j\omega N_o}{D_e + j\omega D_o} \tag{4}$$

The equations and the conditions required for determination of PI stabilization region in the k_p-k_i plane is presented as follows [26], [27]:

For $\omega = 0$
$$k_i = 0 \tag{5}$$

For $\omega \geq 0$
$$k_p = \frac{(\omega^2 N_o D_o + N_e D_e)\cos(\omega\tau) + \omega(N_o D_e - N_e D_o)\sin(\omega\tau)}{-(N_e^2 + \omega^2 N_o^2)} \tag{6}$$

$$k_i = \frac{\omega^2(N_o D_e - N_e D_o)\cos(\omega\tau) - w(N_e D_e + w^2 N_o D_o)\sin(\omega\tau)}{-(N_e^2 + \omega^2 N_o^2)} \tag{7}$$

where $\omega = [0, \omega_c]$

The phase of the system of (1) when $\omega = \omega_c$ is 180º, this condition yielded (8).

$$\tan(\omega\tau) = \frac{\omega(N_o D_e - N_e D_o)}{N_e D_e + \omega^2 N_o D_o} \tag{8}$$

The value of ω_c is the smallest value of ω at which the interception of the graphs of the left- and right-hand sides function of (8) against ω occurred. The PI stability region in the k_p-k_i plane is the area bounded by the line produced by (5) for $\omega = 0$ and the stability locus generated by (6) and (7) for $\omega = [0, \omega_c]$.

2.2. Determination of PI controller gains

Three methods of PI controller gains determination which form the basis for the formulation of the new methods proposed in this study are considered in this section. These methods include GA, CCSR, and WGC which is presented in Subsections 2.2.1, 2.2.2 and 2.2.3 respectively. The objective of the GA is to optimize the PI controller gains (k_p and k_i). The objective of the CCSR is to determine the centroid of the stability region, while the objective of the WGC is to determine the weight of the geometrical center of the stability region.

2.2.1. Determination of PI controller gains via GA

The first step in the design of PI controller for a time-delay systems via GA is to formulate the optimisation constraints from the equations of the stability locus and the real roots line. Optimization of the PI controllers can be achieved by minimizing the objective function. In this study, integral of time multiplied by absolute error (ITAE) shown mathematically in (9) was used as objective function because it gives the best selectivity of the performance indices, it is a good criterion for PID controllers tunning [28] and when system parameters are subject to variations its minimum value is readily discernible [29]:

$$ITAE = \int_0^{T_1} t|e(t)| \, dt \tag{9}$$

where $e(t)$ is the error, t is the time in sec. and $T_1 \geq T_s$,(T_s is the system settling time in sec.).

Selection, crossover, and mutation which are the three reproduction operations used to form new generations in GA optimisation process are briefly explain as follows:

a) Selection: Since the system stability region have been determined, the next step is to randomly select the initial population within the stability region. Evaluation of new generation is done by determining the objective function value for everyone in the population. The fitness function which was obtained by finding the reciprocal of the objective function, is normally used for ranking of the next generation in the population. Individuals are select for reproduction based on their fitness value.

b) Crossover: This is the process by which part of the two parents in this case controller gains selected for the reproduction are combined to form new offspring to improve the next generations,

c) Mutation: To guide against arrival at false optimum controller gains, mutation, which is the act of modifying individual gains in the generation, is applied.

These three reproduction processes will continue until the adopted termination condition is satisfied. Detailed information on PID controller design for system with time delay using GA can be found in [21], [22]. Also, PID controller design for delay free systems is fully discussed in [30].

2.2.2. Determination of PI controller gains using CCSR method

The coordinates of the corner and cusp points of the stability boundary locus were determined. Suppose the number of these corner and cusp points are n and m respectively, then their corresponding coordinates in the k_p-k_i plane can be represented by $(\overline{k}_{p,j}, \overline{k}_{ij,})$ and $(\overline{\overline{k}}_{p,q}, \overline{\overline{k}}_{i,q})$ respectively, $j=1,2,....n$ and $q=1,2,....m.$. The coordinates of the centroid of the convex stability region (k_{pCCSR}, k_{iCCSR}) are the required controller gains in k_p-k_i plane, and they can be calculated by using (10) and (11) respectively [19].

$$k_{pCCSR} = \frac{\sum_{j=1}^{n}\overline{k}_{pj} + \sum_{j=1}^{m}\overline{\overline{k}}_{pj}}{n+m} \tag{10}$$

$$k_{iCCSR} = \frac{\sum_{j=1}^{n}\overline{k}_{ij} + \sum_{j=1}^{m}\overline{\overline{k}}_{ij}}{n+m} \tag{11}$$

2.2.3. Determination of PI controller gains using WGC method

The generated convex stability region is made up of several points which can be defined by unique k_p, k_i coordinates. For m number of points on the stability locus, the k_p, k_i coordinates can be expressed as $(k_{p1}, k_{i1}), (k_{p2}, k_{i2}), \ldots , (k_{pm}, k_{im})$. The stability boundary defined by $k_i = 0$ is independent of ω and gives only real roots, therefore the coordinates of points on this line that corresponds to that on the locus are denoted by $(k_{p1}, 0), (k_{p2}, 0), \ldots , (k_{pm}, 0)$. Each of $(k_{p1}, k_{i1}), (k_{p2}, k_{i2}), \ldots , (k_{pm}, k_{im})$ pair can be mapped to $(k_{p1}, 0), (k_{p2}, 0), \ldots , (k_{pm}, 0)$, respectively.

Note that the value of m is equal to the number of ω steps $(n_{\omega sp})$ and inversely proportional to step size $(\Delta\omega)$. The expression relating $n_{\omega sp}$, ω_c and $\Delta\omega$ is shown in (12). Based on the stability boundary locus and real root boundaries mapping, the controller gains $(k_{pWGC}$ and $k_{iWGC})$ corresponding to WGC point of the system convex stability region can be determined using (13) and (14). This method is simple and can provide good transient performance for systems with time delay [23], [24]. Detailed discussion on WGC technique of PI controller design were reported in [23]-[25].

$$n_{\omega sp} = \frac{\omega_c}{\Delta\omega} \tag{12}$$

$$k_{pWGC} = \frac{1}{m}\sum_{j=1}^{m} k_{pj} \tag{13}$$

$$k_{iWGC} = \frac{1}{2m}\sum_{j=1}^{m} k_{ij} \tag{14}$$

2.3. Proposed methods for PI controller design

In the proposed technique, the controller gains were first obtained using GA, CCSR and WGC methods. Thereafter, the gains obtained from these three methods were now combined by finding the centroids of the lines joining any of the two gain locations, and the triangle whose vertices are the locations of the three gains within the convex stability region. Whichever the case either straight line or triangle, the resultant gains can be obtained by finding respective centroids in the convex stability region.

The four possible centroids in this case are:
a) Centroid of the line joining the location of GA gains and CCSR gains,
b) Centroid of the line joining the location of GA gains and WGC gains,
c) Centroid of the line joining the location of CCSR gains and WGC gains and,
d) Centroid of the triangle whose vertices are the location of GA gains, CCSR gains and WGC gains.

2.4. Time domain-based performance analysis

Performance evaluation of any designed control systems can easily be carried out via simulations. This is achieved in this study by plotting the step response of the controlled and uncontrolled systems on the same axes. Several system TDPMs have been defined for use in assessing system behaviours when the system test signal is a step function. The parameters used in this article include: i) rise time (T_r), ii) peak time (T_p), iii) percentage overshoot (%OS), iv) percentage undershoot (%US), v) settling time (T_s) and vi) steady-state error (ess).

Control system time domain response is made up of two states, namely the transient-state and steady-state responses. The transient-state response depends on system swiftness to the input signal and the degree of closeness of system response to the reference input. The former is characterized by T_r and T_p while the latter is dependent on T_s and %OS. It should be noted that it is not possible to simultaneously satisfy same extreme condition for system swiftness to the input signal and closeness of system response to the reference input. Because these requirements are contradictory in nature, therefore compromise is normally reached to produce the best controller for a given system. The major parameter that is used for characterizing steady-state response is ess.

In the actual sense, selection of controller for a given plant depends on the system performance requirements. If a system is required to reach the set point as fast as possible the controller gains should be selected such that the values of T_r and T_p are as lower as possible. But if tracking the reference input is what is important, then controller gains must be selected such that T_s and %OS are as low as possible. It should also be noted that for good systems steady-state response, ess must be as low as possible.

3.   RESULTS AND DISCUSSIONS

For comprehensive demonstration of the proposed methods, 3 different examples (first, second and third order systems) obtained from [23] were used. Since the steps involved in the PI controller design methods applied in this study are structured, detailed explanation on these steps were only present for Example 1. The detail is not present in Examples 2 and 3 to conserve energy and time. But detailed enough information that can be used for controller performance analysis and comparative analysis among the existing and proposed methds are presented.

3.1. Example 1

A first-order system with time delay was considered. The transfer functions of plant and delay are given in (15) and (16) respectively. Combining (15) and (16) with (3) will yield the system open-loop transfer function from which the closed-loop transfer function can be determined. Based on the closed-loop transfer function the system closed-loop characteristic equation can also be determined.

$$G_p(s) = \frac{1}{s+1} \tag{15}$$

$$G_d(s) = e^{-s} \tag{16}$$

From (2), (4), (15) and (16), $\tau = 1$sec. $N_e = 1$, $N_o = 0$, $D_e = 1$ and $D_o = 1$.

Substituting the values of τ. N_e, N_o, D_e, and D_o into (8) and by letting the left-hand side and right-hand side functions be $f_l(\omega)$ and $f_r(\omega)$ respectively, ω_c can be determined by plotting the two functions against ω as shown in Figure 2. Note that ω_c is defined as the first point of intersection of the two plots, and from Figure 2, $\omega_c = 2.03$ rad/sec. Using (5), (6), and (7), the system stability region of Figure 3 was obtained. It can be seen in Figure 3 that system convex stability region is bounded by the real roots line generated by (5) and the stability locus produced by (6) and (7).

The determination of controller gains for Example 1 using GA was achieved by following the explanation of Subsection 2.2.1 The equation for the system stability locus is a polynomial of 6th-order and it was generated by curve fitting Figure 3, yielding (17) with $R^2 = 0.9998$:

$$k_i = p_1 k_p^{\,6} + p_2 k_p^{\,5} + p_3 k_p^{\,4} + p_4 k_p^{\,3} + p_5 k_p^{\,2} + p_6 k_p + p_7 \tag{17}$$

where: p_1 = -0.030001, p_2 = 0.059705, p_3p3 = 0.011301, p_4p4 = -0.14149, p_5p5 = -0.26956, p_6p6 = 0.93416, p_7 = 1.1352.

The constraints for GA were obtained from (5) and (17) while the objective function was based on the ITAE of (9). The GA was implemented, and the resulting PI controller, that is proportional and integral gains are k_{pGA} = 0.6649 and k_{iGA} = 0.5519 respectively. As earlier explained in Subsection 2.2.2, in this example also, the controller gains at the centroid of system convex stability region were determined. From Figure 4, there are 2 corners and 1 cusp points on the stability boundary locus therefore, n=2 and m =1.
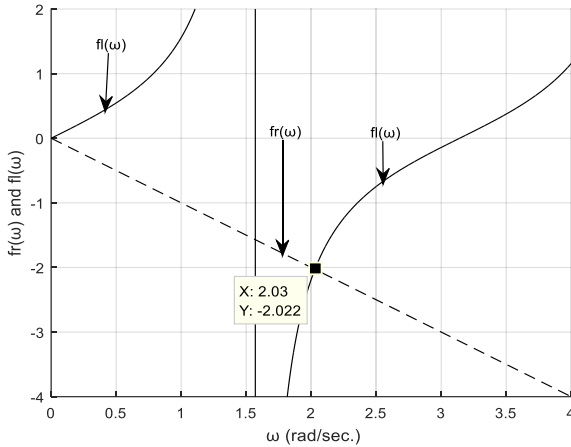
Figure 2. Plots of $f_l(\omega)$ and $f_r(\omega)$ versus ω for Example 1
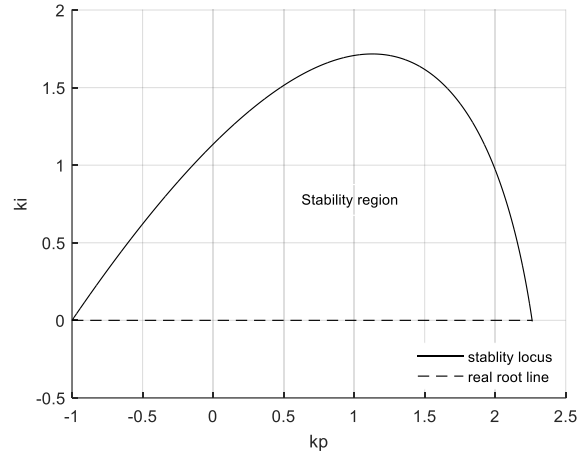
Figure 3. Plot of stability region for Example 1
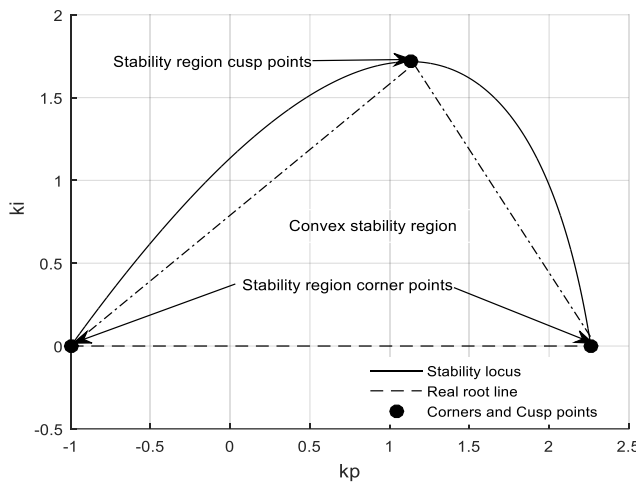
Figure 4. Required points for determination of CCSR for Example 1

The coordinate of the 2 corner points are $(\overline{k}_{p1}, \overline{k}_{i1})$ = (-1, 0) and $(\overline{k}_{p2}, \overline{k}_{i2})$ = (2.263, 0) while that of the cusp point is $(\overline{\overline{k}}_{p1}, \overline{\overline{k}}_{i1})$ = (1.1312, 1.717). Using (10) and (11) the coordinate of the centroid point is (k_{pCCSR}, k_{iCCSR}) = (0.7981, 0.5723). WGC method of PI controller design is presented in Sub section 2.2.3. Considering the generated stability region of Figure 3 and the value of ω_c, $\Delta\omega$ = 0.01 rad/s was selected. Using (12), $n_{\omega sp}$= m=204. Substituting the value of m into (13) and (14) produces the controller gains k_{pWGC} = 0.4442 and k_{iWGC} = 0.4651 at the weighted geometrical centre point of the system stability region. The locations of (k_{pGA}, k_{iGA}) = (0.6649, 0.5519), (k_{pCCSR}, k_{iCCSR}) = (0.7981, 0.5723) and (k_{pWGC}, k_{iWGC}) = (0.4442, 0.4651) are labelled A, B and C in the system stability region as shown in Figure 5, these locations form the vertices of triangle ABC.
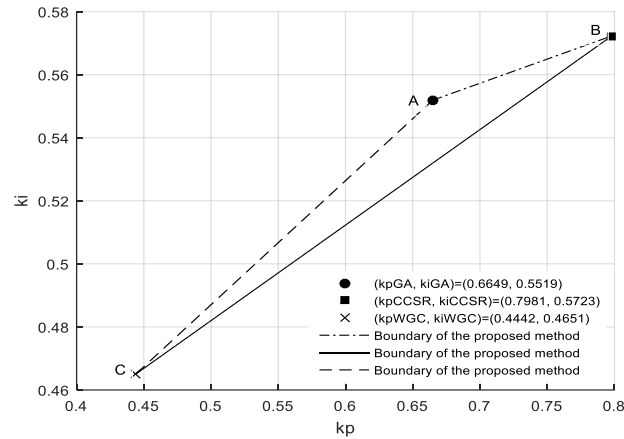
Figure 5. Location of the GA, CCSR and WGC controller gains for Example 1

Based on the coordinate of the vertices of the triangle ABC in Figure 5 and its side lines, the resultant gains at the four possible centroid points were determined by using the steps given in Subsection 2.3. To find the centroid of a line, the number of corners will be 2 and the number of cusps will be 0 that means n =2 and m=0. Also, to find the centroid of triangle the number of corners will be 3 while the number of cusps will be 0 which implies that n =3 and m=0.

The four possible centroid points for this example were determined using (10) and (11) as follows:

a) Centroid of the line that joins the coordinate of GA gains (k_{pGA}, k_{iGA}) = (0.6649, 0.5519) and that of CCSR gains (k_{pCCSR}, k_{iCCSR}) = (0.7981, 0.5723) that is line AB was determined to be (k_{pM1}, k_{iM1}) = (0.7315, 0.5621),

b) Centroid of the line that joins the coordinate of CCSR gains (k_{pCCSR}, k_{iCCSR}) = (0.7981, 0.5723) and that of WGC gains (k_{pWGC}, k_{iWGC}) = (0.4442, 0.4651), line BC was determined to be (k_{pM2}, k_{iM2}) = (0.6211, 0.5187),

c) Centroid of the line that joins the coordinate of GA gains (k_{pGA}, k_{iGA}) = (0.6649, 0.5519) and that of WGC gains (k_{pWGC}, k_{iWGC}) = (0.4442, 0.4651), line CA was calculated and yielded (k_{pM3}, k_{iM3}) = (0.5545, 0.5085) and

d) Finally the centroid of the triangle with vertices defined by the coordinate of GA gains (k_{pGA}, k_{iGA}) = (0.6649, 0.5519), coordinate of CCSR gains (k_{pCCSR}, k_{iCCSR}) = (0.7981, 0.5723) and coordinate of WGC gains (k_{pWGC}, k_{iWGC}) = (0.4442, 0.4651) was also determined to be (k_{pM4}, k_{iM4}) = (0.6357, 0.5298).

The location of all the controller gains of the existing and proposed methods in the system convex stability region are shown in Figure 6. The performance of the proposed method was investigated via simulation. This was achieved by using unit step response of the system. The system was subjected to a unit step function after the incorporation of each of the 7 designed controllers (3 using existing methods and 4 using the proposed methods).
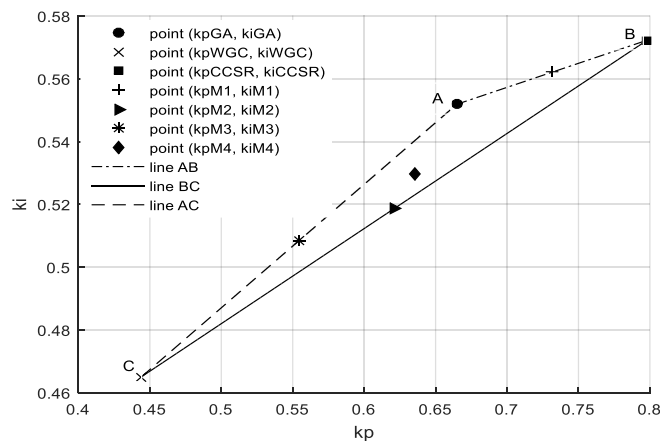

Figure 6. Location of all controller gains in the stability region for Example 1
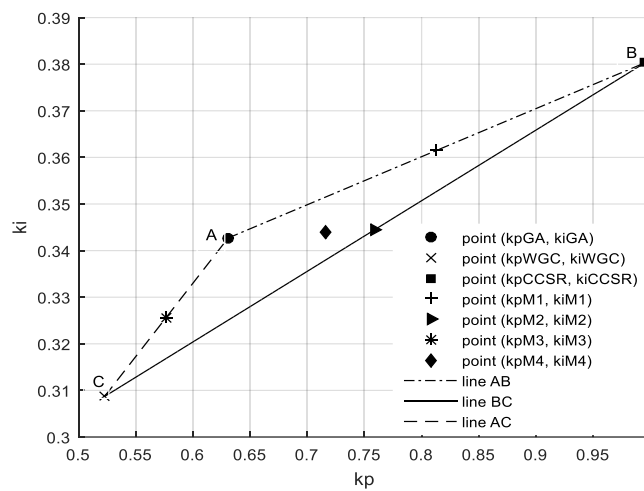
3.2. Discussions of results of Example 1

The determined controller gains using existing and proposed methods for example 1 are shown in Table 1. The corresponding unit step response for this system under the influence of the seven controller design methods and uncontrolled system (UCS) are shown in Figure 7. From Figure 7, the UCS response is far from the reference input, therefore the need for a controller. The required TDPMs for the analysis of the designed system were obtained from Figure 7. The parameters were used for producing the bar chart shown in Figure 8.

Table 1. Existing and proposed methods controller gains for Example 1

$k_p GA$	$k_i GA$	$k_p CCSR$	$k_i CCSR$	$k_p WGC$	$k_i WGC$	$k_p M1$	$k_i M1$	$k_p M2$	$k_i M2$	$k_p M3$	$k_i M3$	$k_p M4$	$k_i M4$
0.6649	0.5519	0.7981	0.5723	0.4442	0.4651	0.7315	0.5621	0.6211	0.5187	0.5545	0.5085	0.6357	0.5298
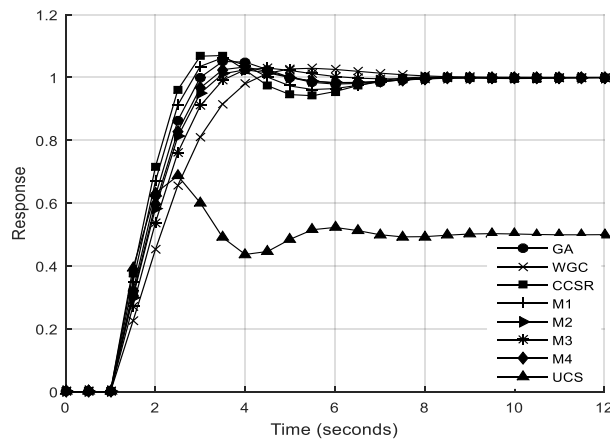
Figure 7. Closed loop unit step response for Example 1

From Figure 8, the minimum and maximum values of T_r were obtained when CCSR and M3 were applied respectively. The minimum and maximum values of T_p corresponds to CCSR and WGC respectively. Also, application of M2 and M1 yielded minimum and maximum values of T_s respectively. But $\%OS$ was minimum when M2 was used and maximum for CCSR. $ess = 0$ for all methods of PI controller design used for this example. Based on these results, it can be inferred that CCSR gives the fastest response and M2 gives the best input tracking response. Since ess=o all the methods have excellent steady-state response.
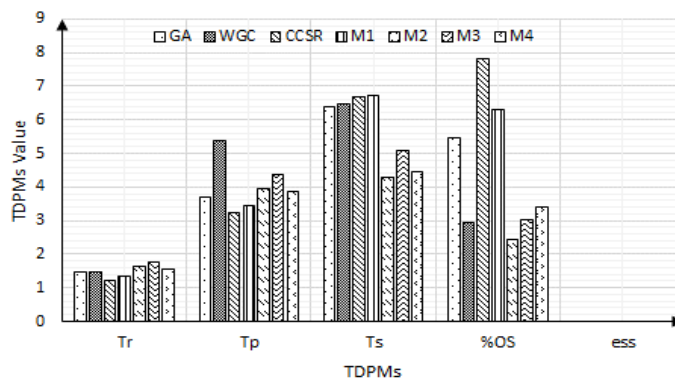
Figure 8. Bar chart for TDPMs and PI design methods for Example 1

As can be clearly seen from Figure 8, compared to GA, M1 gives faster response while M2, M3, and M4 give better reference input tracking. Also, compared to WGC, M1 gives faster response and M2 give better reference input tracking. Lastly, compared to CCSR, methods M2, M3 and M4 produce better reference input tracking.

3.3. Example 2

A second-order system with time delay. The plant and delay transfer functions are as expressed in (18) and (19) respectively:

$$G_p(s) = \frac{1}{(s+1)^2} \tag{18}$$

$$G_d(s) = e^{-s} \tag{19}$$

where from (2) and (19) $\tau = 1$sec. and from (4) and (18) $N_e = 1$, $N_o = 0$, $D_e = 1 - w^2$ and $D_o = 2$.

As done in Example 1, the location of all the controller gains in the stability region using the existing and proposed methods are shown in Figure 9. The performance of the proposed methods was simulated and investigated using system unit step response. The system was subjected to a unit step function after the incorporation of each of the 7 designed controllers (3 using existing method and 4 using the proposed method).

Figure 9. Location of all controller gains in the stability region for Example 2

3.4. Discussions of results of Example 2

The determined controller gains using the existing and proposed methods for Example 2 are shown in Table 2. In this example, the resulting unit step response for the seven controller scenarios understudied is shown in Figure 10. It can be seen from this figure that the response of UCS is far from matching the reference input which call for controller design. The time domain performance parameters associated with each of the controller design methods were obtained from Figure 10 and used for plotting the bar chart of Figure 11.

Table 2. Existing and proposed methods controller gains for Example 2

$k_p GA$	$k_i GA$	$k_p CCSR$	$k_i CCSR$	$k_p WGC$	$k_i WGC$	$k_p M1$	$k_i M1$	$k_p M2$	$k_i M2$	$k_p M3$	$k_i M3$	$k_p M4$	$k_i M4$
0.6308	0.3427	0.9953	0.3803	0.5228	0.3087	0.8131	0.3615	0.7591	0.3445	0.5768	0.3257	0.7163	0.3439

From Figure 11, the minimum and maximum values of T_r correspond to CCSR and M1 respectively. At the same time the minimum and maximum values of T_p are associated with CCSR and WGC respectively. The minimum and maximum values of Ts were obtained using WGC and M4 while the minimum and maximum values of $\%OS$ were realized using WGC and CCSR respectively. The minimum ess was recorded when M1 was used while maximum value was obtained when either GA or M1 was used.

The implication of these results is that the system of Example 2 will have the swiftest response if method CCSR is used but using method WGC will give a system with response that closely track the reference input. The system gives good steady-state response because highest percentage ess obtained was 1.28% which is less than the common standard of 2%. From Figure 11, it can infered that, compared to GA, methods M2,

M3, and M4 yield faster response, while M1 give better reference input tracking. More so, compared to WGC, methods M2, M3, and M4 gives fast response. Lastly, compared to CCSR, M1 gives better reference input tracking.
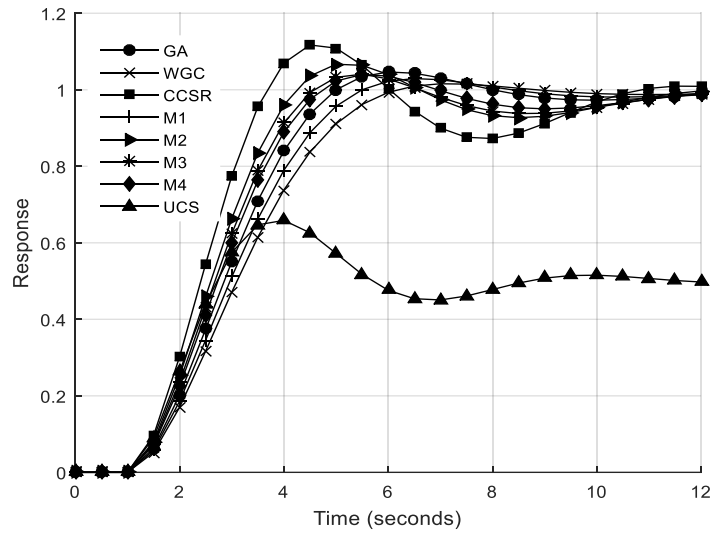
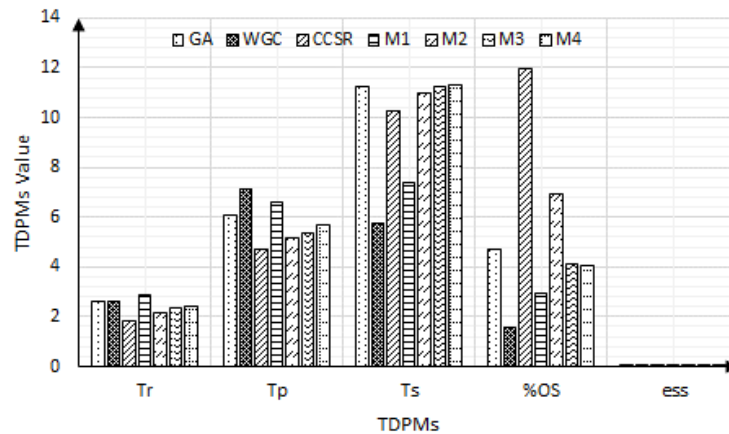

Figure 10. Closed loop unit step response for Example 2

Figure 11. Bar chart for TDPMs and PI design methods for Example 2

3.5. Example 3

Design of PI controller for third-order system with time delay. The plant and delay transfer functions are shown in (20) and (21) respectively.

$$G_p(s) = \frac{1}{(s+1)(s+2)(s+3)} \tag{20}$$

$$G_d(s) = e^{-0.5s} \tag{21}$$

By comparing (2) and (21), $\tau = 0.5$ sec. Also, comparing (4) and (20), $N_e = 1$, $N_o = 0$, $D_e = 6(1 - \omega^2)$ and $D_o = 11 - \omega^2$.

The locations of all the obtained controller gains in the stability region using the existing and proposed methods are shown in Figure 12. The performance of the proposed method was investigated via simulation using system unit step response. The system was subjected to a unit step function after the incorporation of each of the 7 designed controllers (the three existing and four proposed methods).
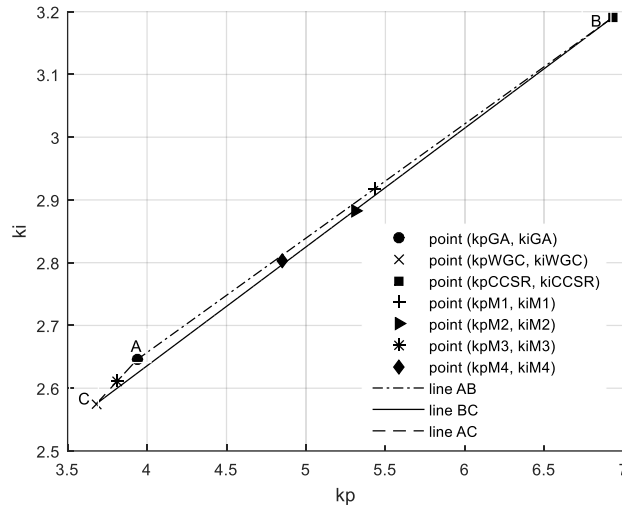
Figure 12. Location of all controller gains in the stability region for Example 3

3.6. Discussions of results of Example 3

Table 3 shows the determined controller gains for the existing and proposed methods for Example 3. The resulting unit step response for Example 3 for the seven controller scenarios is shown in Figure 13. From this figure the response for the UCS is far from getting to the desired output, therefore the system needs a controller. The TDPMs needed for the analysis of this system were obtained from Figure 13. The parameters were used to plot the bar chart of Figure 14.

Table 3. Existing and proposed methods controller gains for Example 3

k_pGA	k_iGA	k_pCCSR	k_iCCSR	k_pWGC	k_iWGC	k_pM1	k_iM1	k_pM2	k_iM2	k_pM3	k_iM3	k_pM4	k_iM4
3.9360	2.6453	6.9330	3.1913	3.6823	2.5755	5.4345	2.9183	5.3076	2.8834	3.8091	2.6104	4.8504	2.8040

From Figure 14 the minimum and maximum values of T_r were obtained when CCSR and M1 was respectively used. Also, the minimum and maximum values of T_p were associated with CCSR and WGC respectively. The minimum and maximum values T_s were realized using WGC and CCSR, while the minimum and maximum values of $\%OS$ were produced using WGC and CCSR respectively. The value of ess was minimum when any out of GA, WGC and M1 was used but maximum when use is made of CCSR.
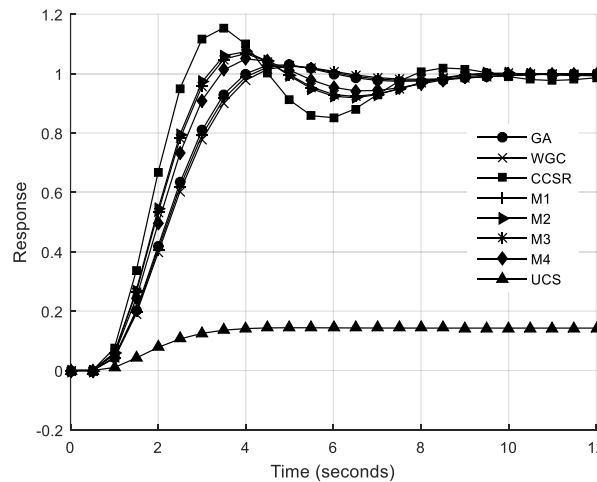
Figure 13. Unit step response for Example 3
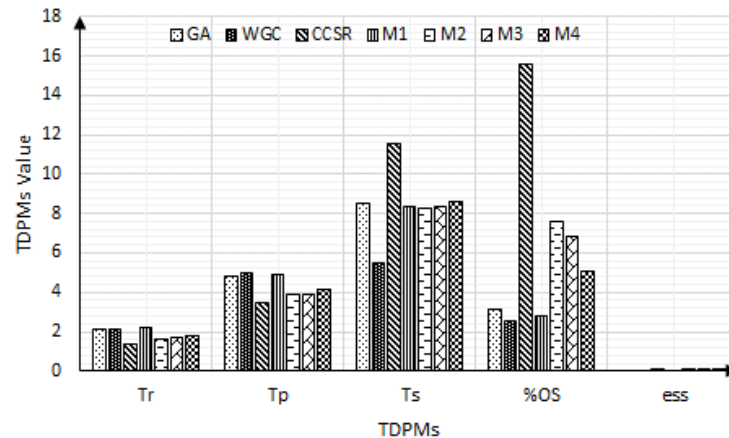
Figure 14. Bar chart for TDPMs and PI design methods for Example 3

The implication of these results is that the system of Example 3 will have the most swiftness response if CCSR method is used but using WGC method will result in a system with response most close to the reference input. Since the maximum percentage *ess* is 1.39% which is less than 2% which is the standard, the steady-state response achieved using any of the controller design methods is good. From Figure 14, when compared to CCSR, methods M2, M3, and M4 gives faster response, while M1 gives better reference input tracking. Furthermore, compared to WGC, methods M2, M3, and M4 give faster response. Finally, compared to CCSR, methods M1, M2, M3, and M4 gives good reference input tracking.

In summary, any of the proposed methods (M1, M2, M3, and M4) can be selected, based on the system performance specifications. It should however be noted that it is not practicable to realize a system that will satisfy all the TDPMs requirements in real life due to their contradicting behavious. Therefore, tradeoffs are normally made once the system performance specification tolerance is known.

4.   CONCLUSIONS

New PI controller design methods for systems with time delay were reported in this study. From the four structured PI controller design methods developed, the selection of any of the methods is informed by the system performance specifications. The system's performance analysis was simplified based on its transient- and steady-state analysis. Satisfactory steady-state responses were obtained in each of the proposed controller design methods since the resulting percentage steady-state error is within the tolerable value (2%). The controlled systems were classified as swift and close reference input tracking according to the resulting system TDPMs. The performance of the controllers realised using few existing methods was tested against the proposed methods via simulation using closed loop unit step response. When compared to any one of the three existing methods, some of the proposed methods yield faster response speed at the expense of reference input tracking, while the reverse is the case for others. Any of the proposed methods (M1, M2, M3, and M4) is a suitable candidate depending on the required system performance specifications. One of the benefits of this study is the creation of pool for PI controller design methods from which selection can be made.

REFERENCES

[1]   S. Testouri, K. Saadaoui, and M. J. Benrejeb, "Robust stabilization of a class of uncertain systems with time delay," *IFAC Proc.*, vol. 43, no. 8, 2010, pp. 553-557, doi: 10.3182/20100712-3-FR-2020.00090.
[2]   L. Barhoumi, I. Saidi, and D. Soudani, "Graphical method for obtaining PID parameters for systems with time delay," *Int. J. Comput. Sci. Netw. Secur.*, vol. 19, no. 7, pp. 31-37, 2019.
[3]   A. Yüce, N. Tan, and D. P. Atherton, "Fractional order pi controller design for time delay systems," *IFAC-PapersOnLine*, vol. 49, no. 10, pp. 94-99, 2016, doi: 10.1016/j.ifacol.2016.07.487.
[4]   J. P. Richard, "Time-delay systems: an overview of some recent advances and open problems," *Automatica*, vol. 39, no. 10, pp. 1667-1694, 2003, doi: 10.1016/S0005-1098(03)00167-5.
[5]   L. M. Eriksson and M. Johansson, "PID controller tuning rules for varying time-delay systems," in 2007 *American Control Conference*, 2007, pp. 619-625, IEEE, doi: 10.1109/ACC.2007.4282655.
[6]   A. Gupta, S. Goindi, G. Singh, H. Saini, and R. Kumar, "Optimal design of PID controllers for time delay systems using genetic algorithm and simulated annealing," in 2017 *International Conference on Innovative Mechanisms for Industry Applications (ICIMIA),* 2017, pp. 66 -69, IEEE, doi: 10.1109/ICIMIA.2017.7975554.
[7]   N. H. Abbas and A. A. Mahmood, "Controller design for gantry crane system using modified sine cosine optimization algorithm," *TELKOMNIKA*, vol. 19, no. 1, pp. 265-276, 2021, doi: 10.12928/TELKOMNIKA.v19i1.17279.

[8]   H. S. Dakheel, Z. B. Abdulla, H. J. Jawad, and A. J. Mohammed, "Comparative analysis of PID and neural network controllers for improving starting torque of wound rotor induction motor," *TELKOMNIKA*, vol. 18, no. 6, pp. 3142-3154, 2020, doi: 10.12928/TELKOMNIKA.v18i6.14571.

[9]   N. J. Hohenbichler, "All stabilizing PID controllers for time delay systems," in *PID Controller Design Approaches - Theory, Tuning and Application to Frontier Areas*, vol. 45, no. 11, pp. 2678-2684, 2009, doi: 10.5772/32293.

[10]   M. B. Shah *et al.*, "PID-based temperature control device for electric kettle," *Int. J. Elect. Comput. Eng.*, vol. 9, no. 3, pp. 1683-1693, 2019, doi: 10.11591/ijece. v9i3.pp1683-1693.

[11]   B. Sumantri, E. H. Binugroho, I. M. Putra, and R. Rokhana, "Fuzzy-PID controller for an energy efficient personal vehicle: Two-wheel electric skateboard," *Int. J. Elect. Comput. Eng.*, vol. 9, no. 6, pp. 5304-5311, 2019, doi: 10.11591/ijece. v9i6.pp5312-5320.

[12]   K. Åström and T. Hägglung, "Introduction," *Advanced PID Control*, ed: International Society of Automation, Chicago, USA, 2006, pp. 64-93. [Online]. Available: https://www.isa.org/products/advanced-pid-control.

[13]   D. F. Putra and A. S. Muharom, "The stability of cannon position on tank prototype using PID controller," *Indones. J. Elect. Eng. Comput. Sci*, vol. 23, no. 3, pp. 1565-1575, 2021, doi: 10.11591/ijeecs.v23.i3.pp1565-1575.

[14]   L. Ou, W. Zhang, and D. J. Gu, "Sets of stabilising PID controllers for second-order integrating processes with time delay," *IEE Proceedings - Control Theory and Applications*, vol. 153, no. 5, 2006, pp. 607-614, doi: 10.1049/ip-cta:20050463.

[15]   H. Efheij and A. Albagul, "Comparison of PID and artificial neural network controller in online of real time industrial temperature process control system," in 2021 *IEEE 1st International Maghreb Meeting of the Conference on Sciences and Techniques of Automatic Control and Computer Engineering MI-STA*, 2021, pp. 110-115: IEEE, doi: 10.1109/MI-STA52233.2021.9464484.

[16]   A. T. Ajiboye, J. O. Popoola, O. Oniyide, and S. L. Ayinla, "PID controller for microsatellite yaw-axis attitude control system using ITAE method," *TELKOMNIKA,* vol. 18, no. 2, pp. 1001-1011, 2020, doi: 10.12928/TELKOMNIKA.v18i2.14303.

[17]   F. Alyoussef and I. Kaya, "A new analytical method for finding the centroid of stability locus for controlling integrating processes," in 2019 IEEE *Int. Conf. Appl. Automat. Ind. Diagnostics*, vol. 1, 2019, pp. 1-6, doi: 10.1109/ICAAID.2019.8934967.

[18]   N. B. Hassen, K. Saadaoui, and M. J. Benrejeb, "Stabilizing lead lag controllers for time delay systems," *Conference: Systems, Control, Signal Processing and Informatics Int. Conf., SCSI'15,* at Barcelone, Spain, vol. 1, no. 2, 2015, pp. 106-109. [Online]. Available: https://www.researchgate.net/publication/299469555_Stabilizing_lead-lag_controllers_for_time_delay_systems.

[19]   C. Onat, "A new design method for PI–PD control of unstable processes with dead time," *ISA Transactions*, vol. 84, pp. 69-81, 2019, doi: 10.1016/j.isatra.2018.08.029.

[20]   F. Alyoussef and I. Kaya, "Tuning proportional-integral controllers based on new analytical methods for finding centroid of stability locus for stable/unstable first-order plus dead-time processes," *Proceedings of the Institution of Mechanical Engineers, Part I: J. Syst. Contr. Eng.*, vol. 236, no. 4, 2022, pp. 818-831, doi: 10.1177/09596518211048028.

[21]   K. Saadaoui, A. Moussa, and M. Benrejeb, "PID controller design for time delay systems using genetic algorithms," *The Mediterranean Journal of Measurement and Control*, vol. 5, no. 1, pp. 31-36, 2009, [Online]. Available: https://www.researchgate.net/publication/271494173_PID_controller_design_for_time_delay_systems_using_genetic_algorithms.

[22]   K. Saadaoui, S. Elmadssia, and M. J. Benrejeb, "Stabilizing PID controllers for a class of time delay systems," in *PID Controller Design Approaches - Theory, Tuning and Application to Frontier Areas*, 2012, pp. 141-158, doi: 10.5772/32293.

[23]   C. Onat, S. E. Hamamci, and S. J. Obuz, "A practical PI tuning approach for time delay systems," *IFAC Proc. Volumes*, vol. 45, no. 14, pp. 102-107, 2012, doi: 10.3182/20120622-3-US-4021.00027.

[24]   M. M. Ozyetkin, C. Onat, and N. Tan, "PI-PD controller design for time delay systems via the weighted geometrical center method," *Asian J. Control*, vol. 22, no. 5, pp. 1811-1826, 2020, doi: 10.1002/asjc.2088.

[25]   C. J. Onat, "A new concept on PI design for time delay systems: weighted geometrical center," *Int. J. Innovative Comput., Inf. Control*, vol. 9, no. 4, pp. 1539-1556, 2013.

[26]   N. Tan, "Computation of stabilizing PI and PID controllers for processes with time delay," *ISA Transactions*, vol. 44, no. 2, pp. 213-223, 2005, doi: 10.1016/s0019-0578(07)90000-2.

[27]   S. Sujoldzic and J. M. Watkins, "Stabilization of an arbitrary order transfer function with time delay using PI and PD controllers," in IEEE 2006 *American Control Conf.*, 2006, pp. 2427-2432, doi: 10.1109/ACC.2006.1656584.

[28]   O. Guenounou, B. Dahhou, and B. Athmani, "Optimal design of PID controller by multi-objective genetic algorithms," in *Int. Conf. Comput. Related Knowledge*, hal-02947644, Sousse, Tunisia, july 2012, pp. 1-6. [Online]. Available: https://hal.archives-ouvertes.fr/hal-02947644/document.

[29]   K. M. Hussain, R. A. R. Zepherin, M. S. Kumar, and S. M. Giriraj Kumar, "Comparison of PID controller tuning methods with genetic algorithm for FOPTD system," *Int. J. Eng. Res. Appl.*, vol. 4, no. 2, pp. 308-314, 2014. [Online]. Available: https://www.ijera.com/papers/Vol4_issue2/Version%201/AT4201308314.pdf.

[30]   A. A. M. Zahir, S. S. N. Alhady, W. A. F. W. Othman, A. A. A. Wahab, and M. F. Ahmad, "Objective functions modification of GA optimized PID controller for brushed DC motor," *Int. J. Elect. Comput. Eng.*, vol. 10, no. 3, pp. 2426-2433, 2020, doi: 10.11591/ijece. v10i3.pp2426-2433.

BIOGRAPHIES OF AUTHORS

Aye Taiwo Ajiboye 🆔 Ⓖ [SC] ↻ is a Reader in the Department of Computer Engineering, University of Ilorin, Ilorin, Nigeria. He obtained a Bachelor of Science degree in Electrical Engineering from the University of Ibadan, Ibadan, Nigeria in 1989, a Master of Engineering degree and a Doctoral degree in Electrical Engineering from University of Ilorin, Ilorin, Nigeria in 2005 and 2012 respectively. He is a Council for Regulation of Engineering in Nigeria (COREN) Registered Engineer and a Member of the Nigerian Society of Engineers (NSE). His research interests have been in Instrumentation and Control Systems design, simulation, and development. He can be contacted at email: ajiboye.at@unilorin.edu.ng.

Jayeola Femi Opadiji is a Reader in the Department of Computer Engineering, University of Ilorin, Ilorin, Nigeria with over twenty years work experience in the academia and the engineering industry. He obtained his Bachelor of Engineering (B.Eng.) and Master of Engineering (M.Eng.) degrees in Electrical Engineering from the University of Ilorin, Nigeria and a Doctor of Engineering (Dr.Eng.) degree in Computer and System Engineering from Kobe University, Japan. Dr. Opadiji is a Council for Regulation of Engineering in Nigeria (COREN) Registered Engineer and a Member of the Nigerian Society of Engineers (NSE). His area of specialization is System Informatics and his research interests cut across optimization of complex systems, multiagent systems, industry 4.0 and science and engineering education. He can be contacted at email: jopadiji@unilorin.edu.ng.

Abdulrahman Olalekan Yusuf received the B.Eng. degree in Electrical/ Electronic Engineering from Federal University of Technology Minna, Nigeria, the M.Eng. degree in Electrical and Electronics Engineering from the University of Ilorin, Ilorin, Nigeria. He is a lecturer in the Department of Computer Engineering, University of Ilorin, Ilorin Nigeria. His research interests include embedded systems, robotics and software engineering. He can be contacted at email: yusuf.oa@unilorin.edu.ng.

Olusogo Joshua Popoola is a Research Fellow in the Department of Computer Engineering, University of Ilorin, Ilorin, Nigeria. He obtained his Bachelor of Engineering (B.Eng.) degree in Electrical and Electronics Engineering from the University of Ilorin, Nigeria in 1995 and Master of Science (M.Sc.) degree in Computer and Network Engineering from Sheffield Hallam University, United Kingdom in 2017. He has over twenty years of experience, great passion for and interest in electronics, control systems, digital communication, and digital information throughput (IP Network Engineering). He is also a researcher in computing and informatics, committed to continuous improvement in IoT cryptography systems. He is a Council for Regulation of Engineering in Nigeria (COREN) Registered Engineer and a Member of the Nigerian Society of Engineers (NSE). He can be contacted at email: olusogo@unilorin.edu.ng.
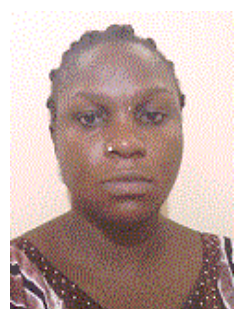
Esther Toyin Olawole received her B.Eng. and M.Eng. degrees in Electrical and Electronics Engineering in 2010 and 2016, respectively, from University of Ilorin, Ilorin, Kwara State, Nigeria. She is currently pursuing her Ph.D. degree at Ladoke Akintola University of Technology, Ogbomosho, Oyo State. Nigeria. She is a Technologist in the Department of Computer Engineering, University of Ilorin, Kwara State, Nigeria. Her research interests are in signal processing in wireless communication. She can be contacted at email: olawole.et@unilorin.edu.ng.

Olalekan Femi Adebayo received the B.Eng. degree in Electrical/Electronic Engineering from the University of Ilorin, Nigeria, and the M.Eng. degree in Electrical and Electronics Engineering from the University of Ilorin, Ilorin, Nigeria. He is an Academic Technologist in the Department of Computer Engineering, University of Ilorin, Ilorin Nigeria. His research interests include Network Security and software engineering. He can be contacted at email: adebayo.of@unilorin.edu.ng.